LUNG CANCER DETECTION USING CHAN-VESE MODEL

Sanjana Srinath, Sushma Ganesh, Vishal B, Syed Daanish, Dr A B Rajendra

Department of Information Science & Engineering

Vidyavardhaka College of Engineering, Mysuru

Abstract

CT images and the detailed analysis of these images have become seemingly important for many reasons, including lung parenchyma density analysis, airway analysis, diaphragm mechanics analysis, and nodule detection for cancer screening. The important prerequisite for automatic image segmentation is Lung segmentation. Here, we propose a method for lung segmentation and to minimize the juxta plural nodule issue.

Keywords ***Lung segmentation, juxta-pleural nodule, CT images***

I. BACKGROUND

Chest computed tomography images and their analysis have become increasing popular in the field of medicine to solve variety of problems such as pneumonia, diagnosis of cancer by detecting nodules, unexplained cough, shortness of breath and many more. Segmentation of lung is a major prerequisite for automated image analysis. Various algorithms are applied to identify patterns and gather information for data analysis. Presence of pulmonary nodules are the major indicators of cancer. Juxta-pleural nodule present at the pleural surface of the chest. Their presence makes it difficult to decide the boundaries between the surfaces as shown in the figure below.

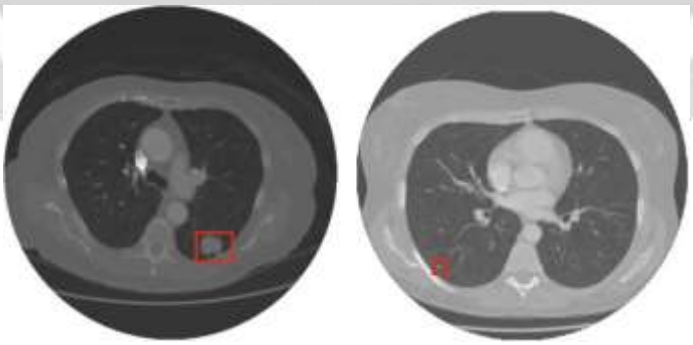

Fig 1. Presence of Juxtapleural nodule

Different methods are used for detecting the nodules and segmenting the lungs most of them using edge detection or snake methods.

II. IMPLEMENTATION

We propose a system that uses Chan Vese model for segmentation of lung contour along with bayesian approach for the juxta-plueral nodules. This is on the assumption that contours are expanded or contracted over frames. The lung contour is predicted

and updated over multiple frames. The changes amongst Bayesian model and CV are extracted as groups. These images were investigated to concluded if they were nodules or parts of lung using circle/ellipse Hough transform and concave point detection. Our proposed method was compared with CV, normalized and modified CV and snake method to evaluate our performance.

A. COLLECTION OF CT SCAN IMAGES

We collected CT diacom images of 84 anonymous subjects out of which 42 were with juxta-pleural nodules. There were around 16,873 images in total out of which 314 was the case of juxta-pleural nodules. Each scan consisted of 105-210 image frames.

B. LUNG CONTOUR EXTRACTION WITH CV MODEL

CV model is applied to CT images of chest. Ω is the bounded open subset of R^2 with the boundary $\partial\Omega$. C is lung contour, *inside(C)* and *outside(C)* denote the regions w and $\Omega\backslash\overline{ww}$, respectively. the energy term F^G is defined by

$$\begin{aligned} F^G(c_1,c_2,C) = &\mu \cdot Length(C) + \nu \cdot Area(inside(C)) \\ &+ \lambda_1 \int_{inside(C)} |u_0(x,y) - c_1|^2 \, dxdy \\ &+ \lambda_2 \int_{outside(C)} |u_0(x,y) - c_2|^2 \, dxdy \end{aligned}$$

where $\mu \geq 0$, $\nu > 0$, $\lambda_1, \lambda_2 > 0$ are fixed parameters. *Length(C)*- length of the lung contour C $u_0(x,y)$ pixel intensity in Ω. curve C is then found to minimize the global energy term F^G as

$$\inf_{c_1,c_2,C} F^G(c_1,c_2,C)$$

To find the solution for C, the level set method is used, which replaces the unknown contour C by the level set function $\Phi(x,y)$. Then

$$\begin{aligned} F^G = &F^G(c_1,c_2,\emptyset) = \mu \int_\Omega \delta(\emptyset(x,y)) |\nabla \emptyset(x,y)| \, dxdy \\ &+ \nu \int_\Omega H(\emptyset(x,y)) dxdy + \lambda_1 \int_{inside(C)} |u_0(x,y) \\ &- c_1|^2 H(\emptyset(x,y)) dxdy + \lambda_2 \int_{outside(C)} |u_0(x,y) \\ &- c_2|^2 (1 - H(\emptyset(x,y))) \, dxdy \end{aligned}$$

Heaviside function $H(z)$ is one if $z \geq 0$ and zero if $z < 0$. For numerical approximation of the model, the Heaviside function is slightly regularized as

$$H_\varepsilon(z) = \frac{1}{2}\left(1 + \frac{2}{\pi}\arctan\left(\frac{z}{\varepsilon}\right)\right)$$

c_1 and c_2 were updated for the initial curve C.

$$\varphi(X) = \sin\left(\frac{\pi}{5}x\right)\sin\left(\frac{\pi}{5}y\right)$$

After applying with CV model, nodules inside parenchyma are segmented. To separate them form contours, two longest contours are selected corresponding to left and right lungs.

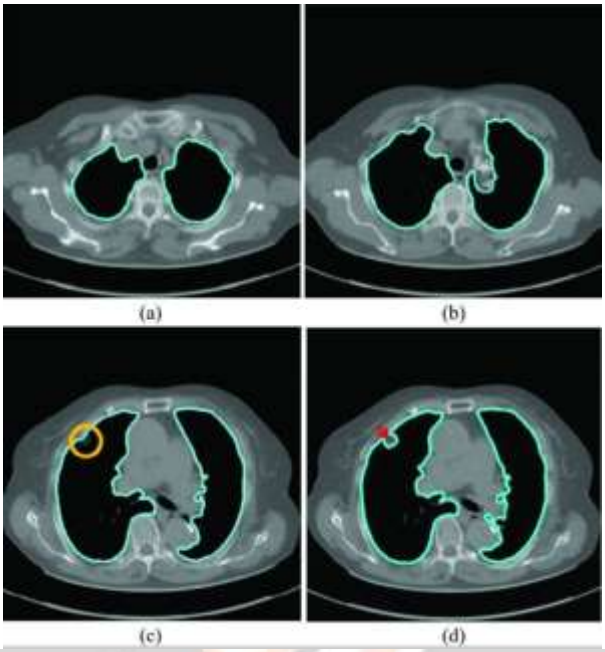

Fig 2A.(a) and (b) Most contours segmented.

(c) Segmented with nodules. (d) Segmented without nodules.

B. Bayesian Approach

Given N successive chest CT image frames, lung contour state vector of the n-th image is denoted by C_F^n, where

$$C_F^n = f_n(C_F^{n-1}, w^n)$$

We need to construct the PDF of the state vector C_F^n ,given all the available information of $p(C_F^n|D^n)$, it can be obtained recursively in two stages of prediction and update. Given the PDF and based on Markov model, $p(C_F^n|C_F^{n-1})$ can be formulated as

$$p(C_F^n|C_F^{n-1}) = \int \delta(C_F^n - f_n(C_F^{n-1}, w^n))p(w^n)dw^n$$

the prior PDF for the posterior PDF can be updated via the Bayes rule as $p(C_F^n|D^n) = \frac{p(C_G^n|C_F^n)\,p(C_F^n|D^{n-1})}{p(C_G^n|D^{n-1})}$

normalizing the denominator and defining by measurement functions

$$p(C_G^n|C_F^n) = \int \delta(C_G^n - h_n(C_F^n, v^n))p(v^n)dv^n$$

Prediction Stage: Given the contour C_F^{n-1}, we formed the prior $p\{C_F^n|D^{n-1}\}$ by dilating and contracting C_F^{n-1} as shown in Fig 2B(a). The blue areas are dilated curve samples, and the red areas are contracted curve samples. The dilated curves were sampled moving each pixel of C_F^{n-1} toward the normal vector, and the contracted curves were sampled moving each of C_F^{n-1} toward the opposite normal vector. Each pixel movement for dilation and contraction was from 1 to 5 pixels. predicted curve samples denoted by $C_F^{*n(i)}$.

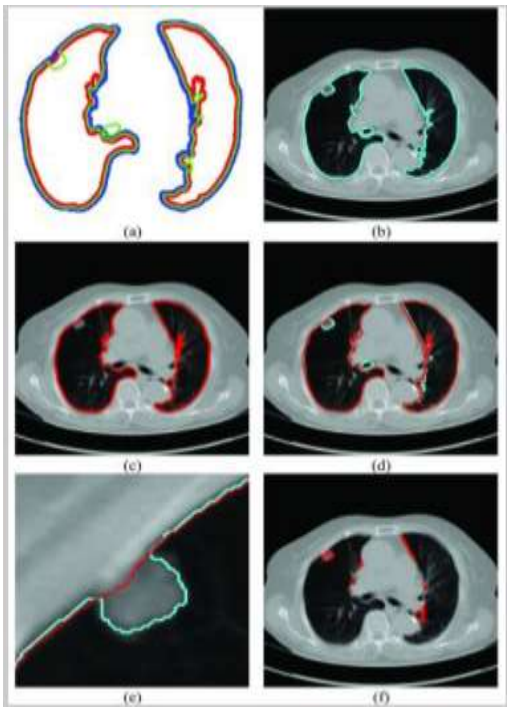

Fig 2B (a) Curve samples for dilation(blue) and contraction(red). (b) global contour. (c) contours providing highest correlation value. (d)overlapped contours (e) enlarged and highlighted nodules. (f) resultant juxta-pleural nodules

Update Stage: The best fitted prediction curve was found by evaluating cross correlation. The updated contour sample C_F^{*n} provided the highest correlation values for the left and right lungs. Next the difference image from result of Bayesian approach and CV model were found by simultaneously finding segments outside the contour C_G^n and inside the contour C_F^{*n}.

The separated segments are juxta-pleural nodule candidates.

C. ELIMINATION OF FALSE POSITIVES

Inorder to classify the nodules as True or False positive, it is necessary to find out if each candidate contour included any concave point from the centre point of C_G^n. the set of contour points of each nodule candidate is denoted by

$$\boldsymbol{P}_c^{n(i)} = \left\{ P_c^{n(i,j)} : j = 1,2,\ldots J \text{ and } i = 1,2,\ldots I \right\},$$

the included angle $\angle OP_c^{n(i,j)}Q$, and declared the point $P_c^{n(i,j)}$ was calculated to be a concave point if the angle was less than 90. the resultant angles are denoted by θ_{in} and θ_{out}.

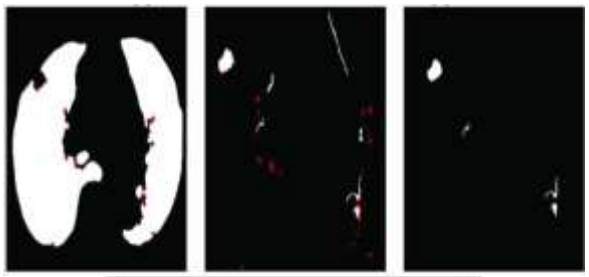

(a) (b) (c)

Fig 2C(i). (a) detected concave points with red dots on C_G^n. (b) detected concave points on nodule candidate contours (c)remaining nodule candidates including concave points

In the last step circle/ ellipse shape segments were found amongst the remaining nodules using circular Hough transform. The similarity metric S for each segment is calculated considering only segments with $S \geq S_{TH}$, where $S_{TH} = 0.49$, which was optimized using the receiver operating characteristic (ROC) curve.

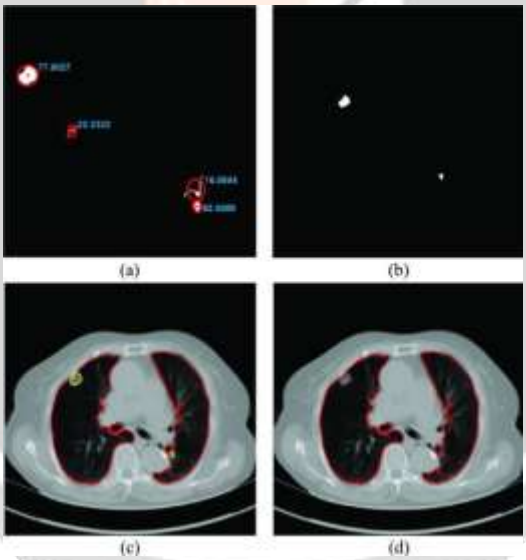

Fig 2C(ii) (a) similarity metric for each segment. (b) two remaining segments with metric value greater than 0.49 (c) Area of remaining segments (yellow contours) added to area inside C_G^n.

(d) modified lung contour by adding the nodule candidates to the area inside C_G^n

D. PERFORMANCE EVALUATION

To evaluate performance five metrics are considered; the disc similarity coefficient (DSC), modified Hausdorff distance (MHD), sensitivity, specificity, and accuracy. For this, true positive (TP), false positive (FP), true negative (TN), and false negative (FN) should be calculated. TP – number of positive pixels labelled correctly whereas FP is ones labelled incorrectly. TN- number of negative pixels labelled correctly whereas FN is ones labelled incorrectly. Example is shown below.

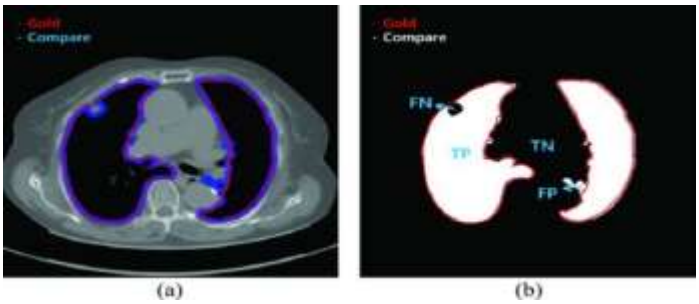

Fig 2D (a) Gold standard(purple) and estimated contour(blue). (b) Corresponding TP,FP,TN and FN

Based on these 4 parameters the DSC is

$$DSC = \frac{2TP}{2TP + FP + FN}$$

DSC is used for determining segmentation of false positives and false negatives. The value ranges from 0 to 1, 0 means no similarity and 1 means perfect similarity. MHD measures how far two subsets are from each other. Other metrics are calculated as

$$\text{Sensitivity} = \frac{TP}{TP + FN}$$

$$\text{Specificity} = \frac{TN}{TN + FP}$$

$$\text{Accuracy} = \frac{TP + TN}{TP + TN + FP + FN}$$

To evaluate the proposed method, results of CV, NM-CV, snake algorithm was compared with our method.

III. RESULTS

To asses our method CT digital imaging and communication in medicine images of 84 anonymous subjects and 42 juxta-pleural cases were collected. Out of a total of 16873 images 314 were juxta-pleural cases. Our method exhibited a disc similarity coefficient of 0.9809, modified hausdorff distance of 0.4806, sensitivity of 0.9785, specificity of 0.9981, accuracy of 0.9964, and juxta-pleural nodule detection rate of 96%. It outperformed existing methods as shown in table below.

TABLE 1

Result of comparison on all four methods on CT images

METHOD		**CV**	**NMCV**	**SNAKE**	**PROPOSED METHOD**
DSC	mean	0.9692	0.9693	0.9684	0.9709
	std	0.0524	0.0513	0.0514	0.0511
MHD	mean	0.5191	0.5162	0.5227	0.5006
	std	0.5978	0.5837	0.5927	0.5771
Sensitivity	mean	0.9550	0.9554	0.9543	0.9585
	std	0.0728	0.0722	0.0746	0.0722
Specificity	mean	0.9992	0.9991	0.9993	0.9981
	std	0.0015	0.0013	0.0017	0.0012

Accuracy	mean	0.9952	0.9953	0.9951	0.9954
	std	0.0129	0.0128	0.0132	0.0129

IV. CONCLUSION

The above proposed paper has the capability of detecting juxta-pleural nodule. The algorithm is based on chan-vese model followed by Bayesian approach and eliminate false positives through concave points detection and circle/ellipse Hough transform. We believe that our proposed method enhances the accuracy of lung segmentation and can assist radiologists in the interpretation of CT images, particularly for lung-related quantitative analysis.

REFERENCES

[1] Jiang X., Zhang R., and Nie S., "Image segmentation based on level set method," *Phys. Procedia*, vol. 33, pp. 840–845, 2012.

[2] Chopin J. P., Miklavcic S. J., and Laga H., "Selection of parameters in active contours for the phenotypic analysis of plants," in *Proc. 20th Int. Congr. Modelling Simulation*, 2013, pp. 510–516.

[3] Mansoor A.et al., "Segmentation and image analysis of abnormal lungs at CT: Current approaches, challenges, and future trends," *RadioGraphics*, vol. 35, no. 4, pp. 1056–1076, 2015.

[4] Getreuer P., "Chan-vese segmentation," *Image Process. Line*, vol. 2, pp. 214–224, Aug. 2012.